Drift chambers

(First studies: T. Bressani, G. Charpak, D. Rahm, C. Zupancic, 1969
First operation drift chamber: A.H. Walenta, J. Heintze, B. Schürlein, NIM 92 (1971) 373)

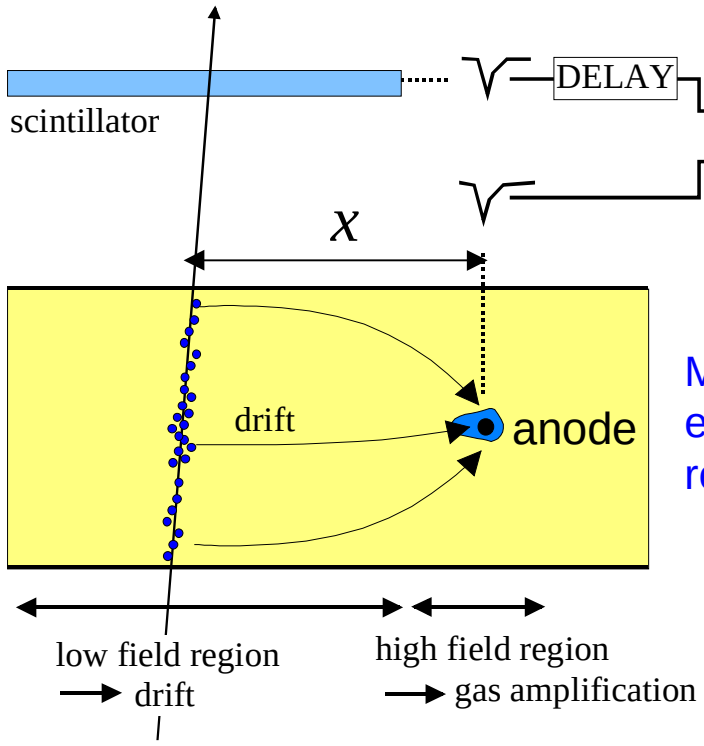

Measure arrival time of electrons at sense wire relative to a time t_0.

$$x = \int v_D(t)dt$$

What happens during the drift towards the anode wire ?

- Diffusion ?
- Drift velocity ?

Drift and diffusion in gases

No external fields:

Electrons and ions will lose their energy due to collisions with the gas atoms → thermalization

$$\varepsilon = \frac{3}{2} kT \approx 40 \text{ meV}$$

Undergoing multiple collisions, an originally localized ensemble of charges will diffuse

$$\frac{dN}{N} = \frac{1}{\sqrt{4\pi Dt}} e^{-(x^2/4Dt)}\, dx$$

D: diffusion coefficient

$$\sigma_x(t) = \sqrt{2Dt} \quad or \quad D = \frac{\sigma_x^2(t)}{2t}$$

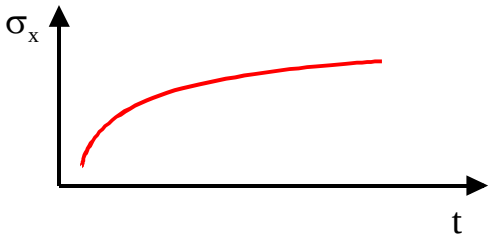

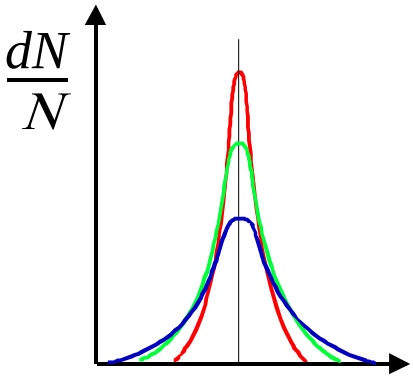

External electric field:

"stop and go" traffic due to scattering from gas atoms

→ drift

$$\vec{v}_D = \mu \vec{E} \qquad \mu = \frac{e\tau}{m} \text{ (mobility)}$$

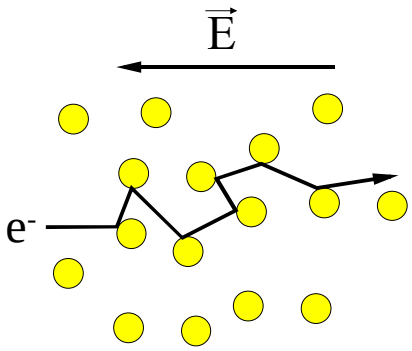

in the equilibrium ... $\frac{x}{v_D \tau} \lambda_\varepsilon \varepsilon = eEx$

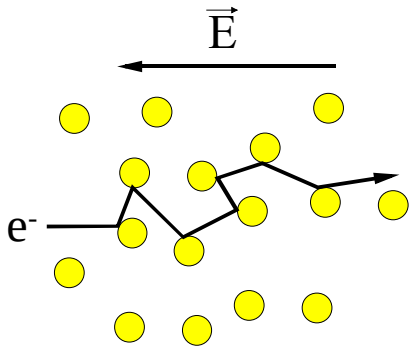

λ_ε : fractional energy loss / collision

$\tau = \frac{1}{N\sigma v}$ v: instantaneous velocity

$$\rightarrow \quad v_D^2 = \frac{eE}{mN\sigma}\sqrt{\frac{\lambda}{2}}$$

$\sigma = \sigma(\varepsilon)$!

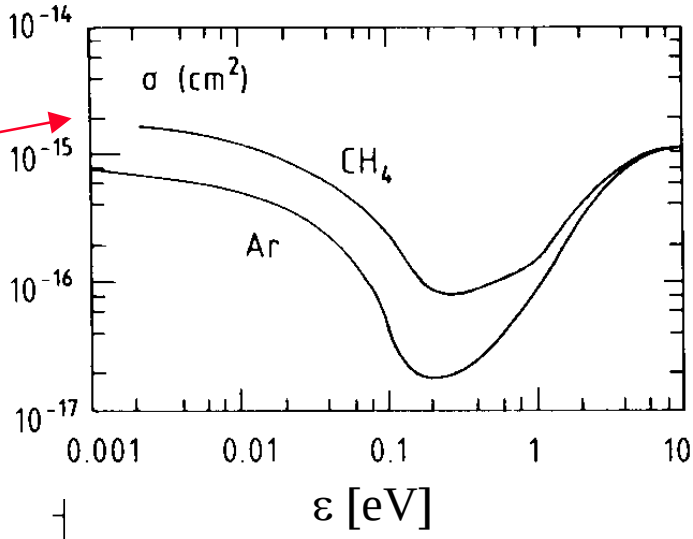

(B. Schmidt, thesis, unpublished, 1986)

$\lambda = \lambda(\varepsilon)$!

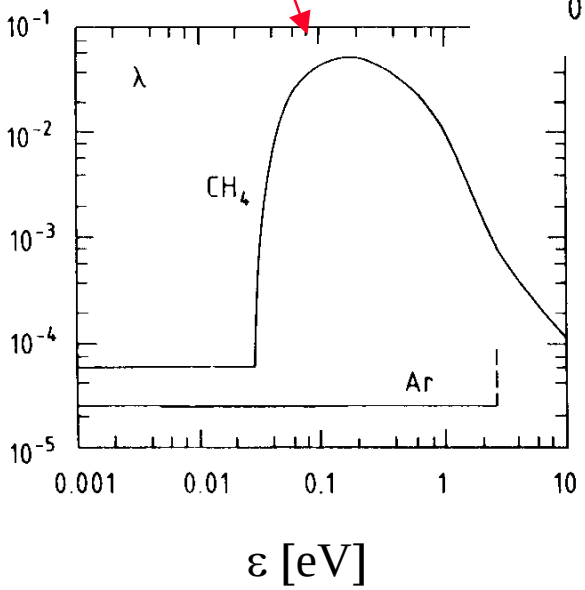

Typical electron drift velocity: **5 cm/μs**

Ion drift velocities: ca. 1000 times smaller

In the presence of electric and magnetic fields, drift and diffusion are driven by $\vec{E} \times \vec{B}$ effects

Look at 2 special cases:

Special case: $\vec{E} \perp \vec{B}$

$\tan \alpha_L = \omega \tau$

α_L: Lorentz angle

$\omega = \frac{e\vec{B}}{m}$ cyclotron frequency

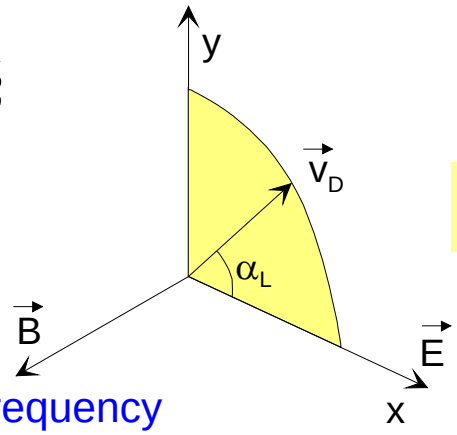

$\vec{v}_D \nparallel \vec{E}$

Special case: $\vec{E} \parallel \vec{B}$

The longitudinal diffusion (along B-field) is unchanged.
In the transverse projection the electrons are forced on circle segments with the radius v_T/ω.
The transverse diffusion coefficient appears reduced

$$D_T(B) = \frac{D_0}{1+\omega^2\tau^2}$$

Very useful… see later !

Transverse diffusion σ (μm) for a drift of 15 cm in different Ar/CH_4 mixtures

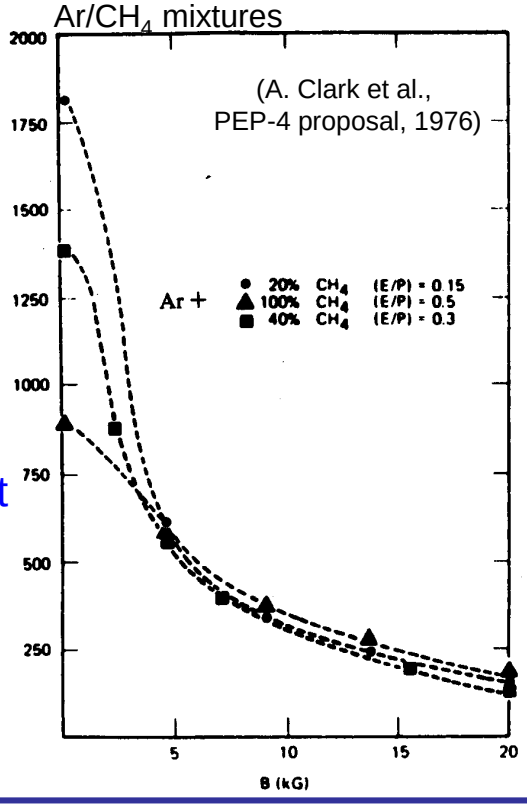

Some planar drift chamber designs

Optimize geometry → constant E-field
Choose drift gases with little dependence $v_D(E)$
→ linear space - time relation r(t)

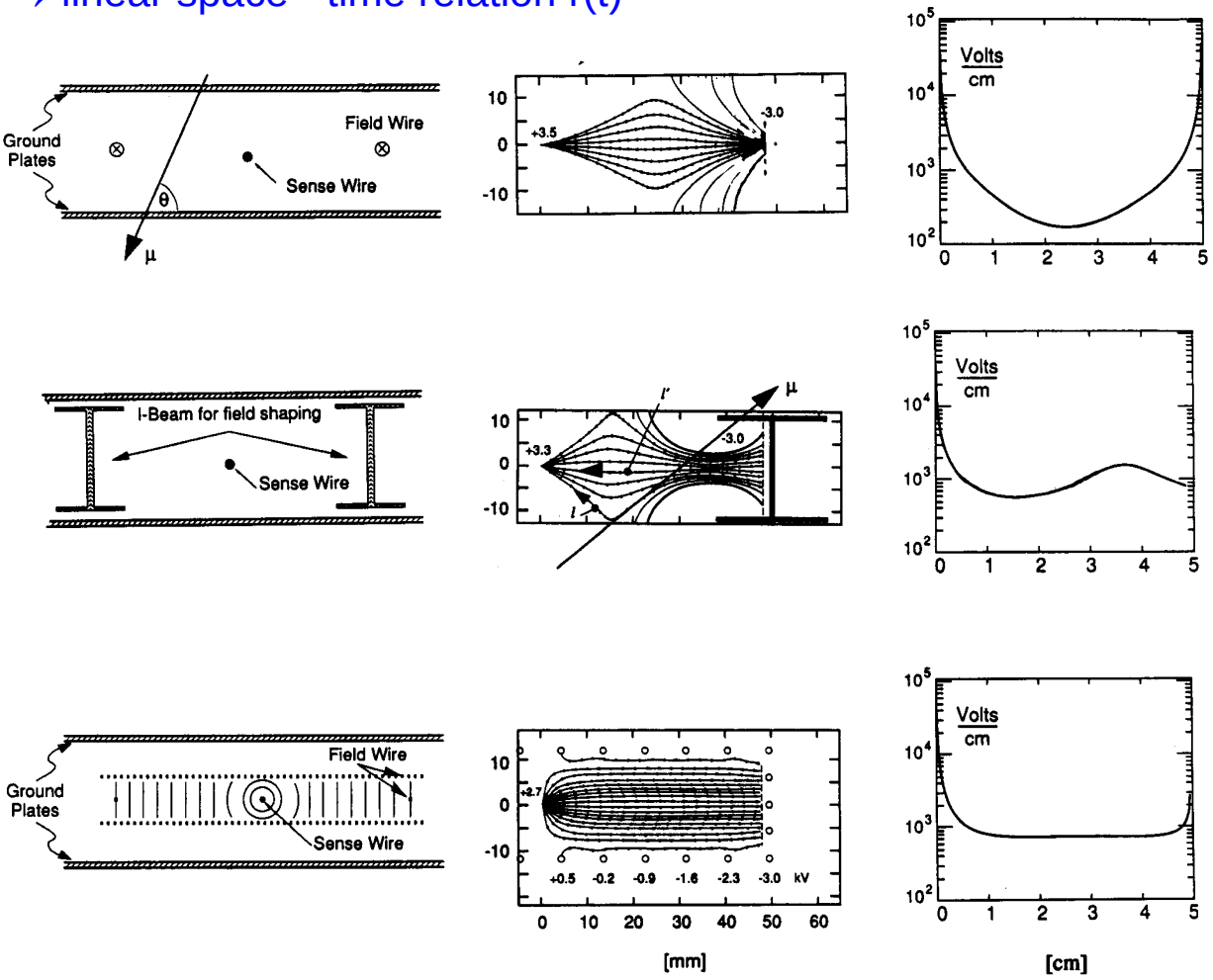

(U. Becker, in: Instrumentation in High Energy Physics, World Scientific)

The spatial resolution is not limited by the cell size
→ less wires, less electronics,
less support structure than in MWPC.

Resolution determined by
- diffusion,
- path fluctuations,
- electronics
- primary ionization statistics

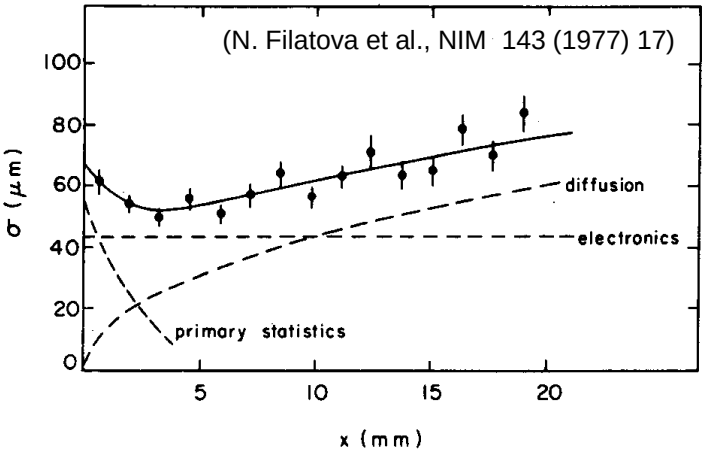

Various geometries of cylindrical drift chambers

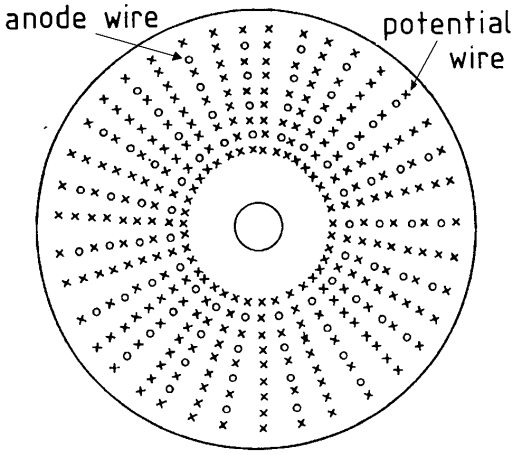

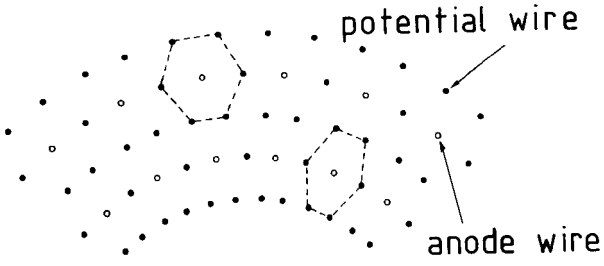

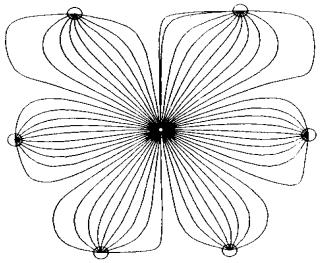

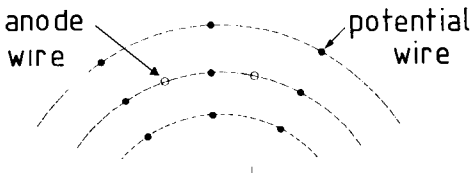

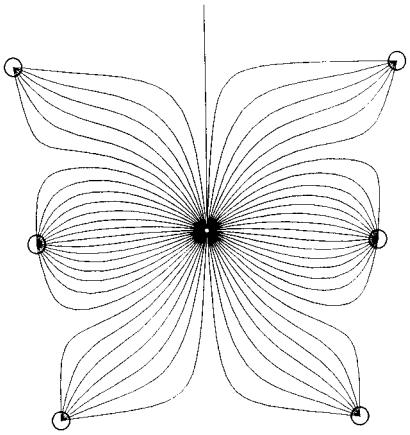

Straw tubes: Thin cyclindrical cathode, 1 anode wire

principle

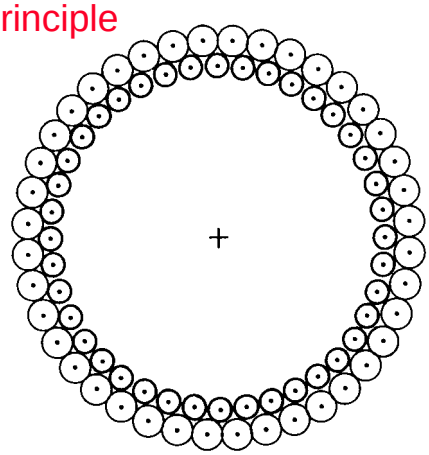

Example: DELPHI Inner detector

5 layers with 192 tubes each
tube ∅ 0.9 cm, 2 m long,
wall thickness 30 μm (Al coated polyester)
wire ∅ 40 μm
Intrinsic resolution ca. 50 μm

Jet chambers: Optimized for maximum number of measurements in radial direction

principle

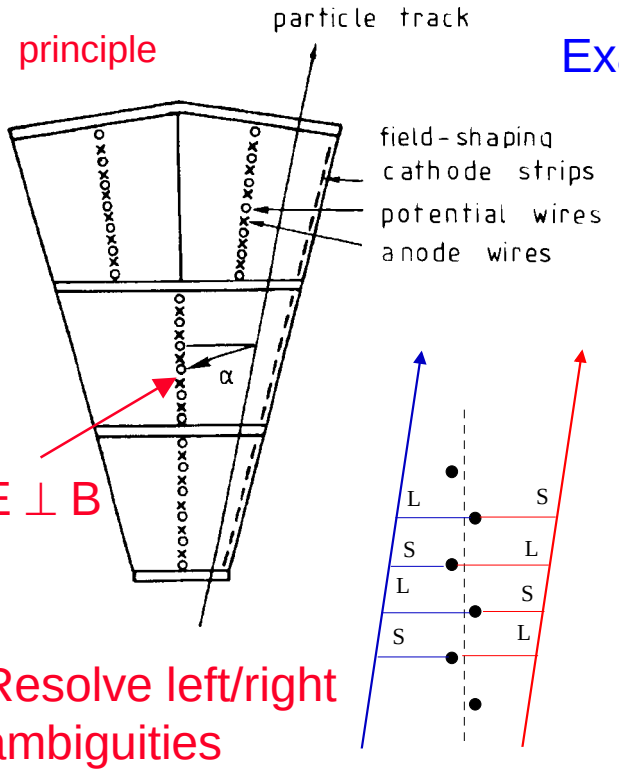

Resolve left/right ambiguities

Example: OPAL Jet chamber

Ø=3.7m, L=4m, 24 sectors à 159 sense wires (±100 μm staggered). 3 cm < l_{drift} < 25 cm

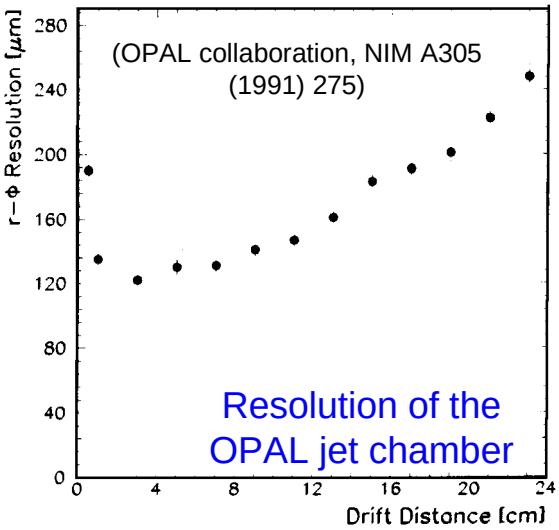

Resolution of the OPAL jet chamber

Time Projection Chamber → full 3-D track reconstruction

- x-y from wires and segmented cathode of MWPC
- z from drift time
- in addition dE/dx information

PEP-4 TPC

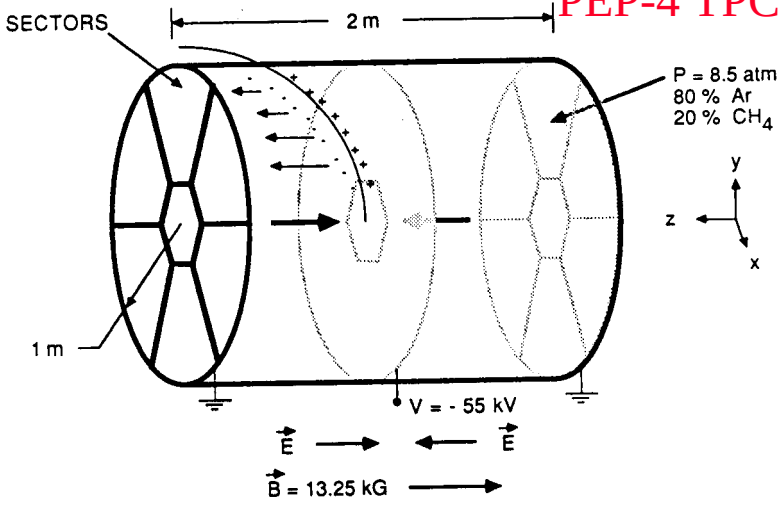

Diffusion significantly reduced by B-field.

Requires precise knowledge of v_D → LASER calibration + p,T corrections

Drift over long distances → very good gas quality required

Space charge problem from positive ions, drifting back to midwall → gating

ALEPH TPC

(ALEPH coll., NIM A 294 (1990) 121,
W. Atwood et. Al, NIM A 306 (1991) 446)

Ø 3.6M, L=4.4 m

$\sigma_{R\phi} = 173\ \mu m$
$\sigma_z = 740\ \mu m$
(isolated leptons)

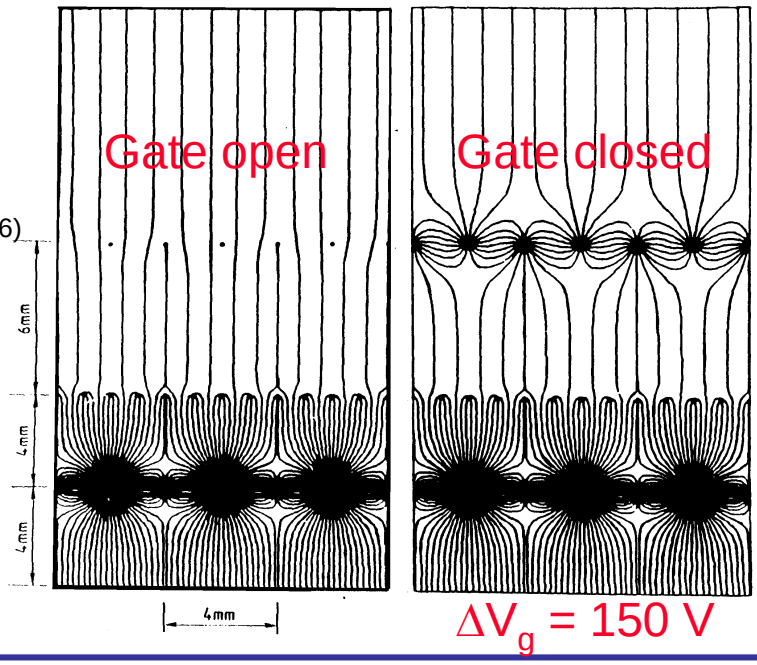

$\Delta V_g = 150$ V

Faster and more precision ? → smaller structures

◆ Microstrip gas chambers

(A. Oed, NIM A 263 (1988) 352)

geometry and typical dimensions (former CMS standard)

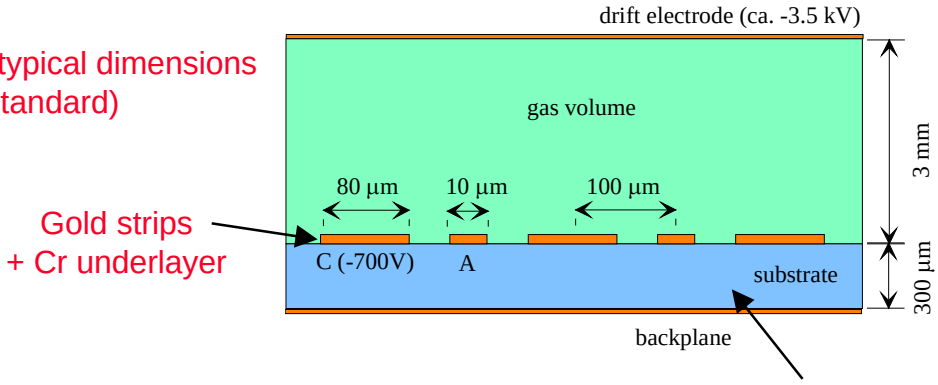

Glass DESAG AF45 + S8900 semiconducting glass coating, $\rho = 10^{16}\ \Omega/\square$

Field geometry

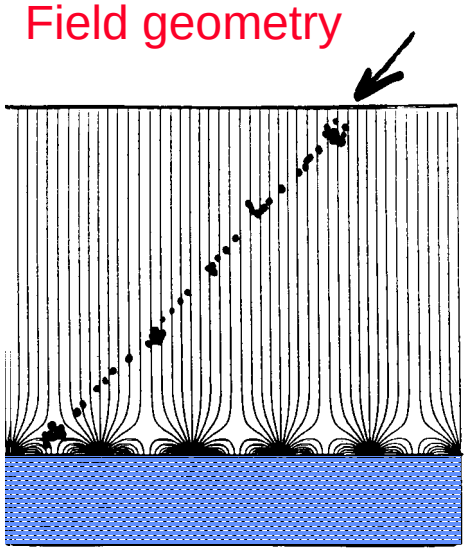

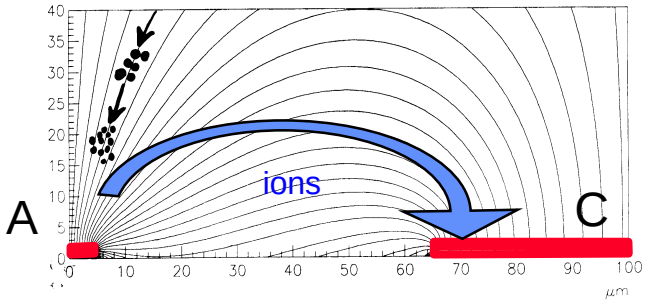

Fast ion evacuation → high rate capability
≈ 10^6 /(mm²·s)

Gas: Ar-DME, Ne-DME (1:2), Lorentz angle 14º at 4T, CMS

Gain ≤10^4

Passivation: non-conductive protection of cathode edges

Resolution: ≈ 30..40 µm

Aging: Seems to be under control.
10 years LHC operation ≈ 100 mC/cm

Micro gap chambers

F. Angelini, NIM A 335 (1993) 69

INFN Pisa

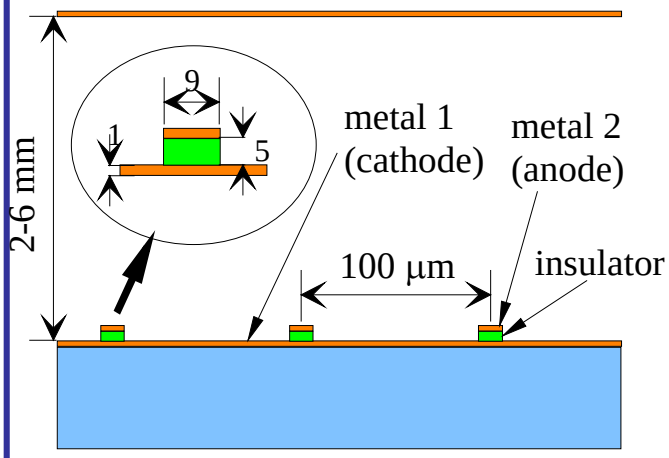

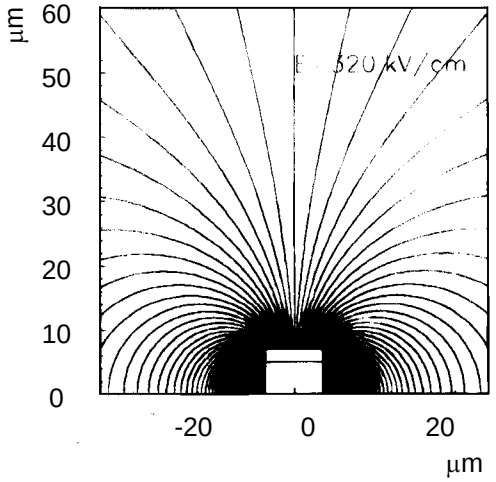

2-dimensional readout with MGC (Bellazini)

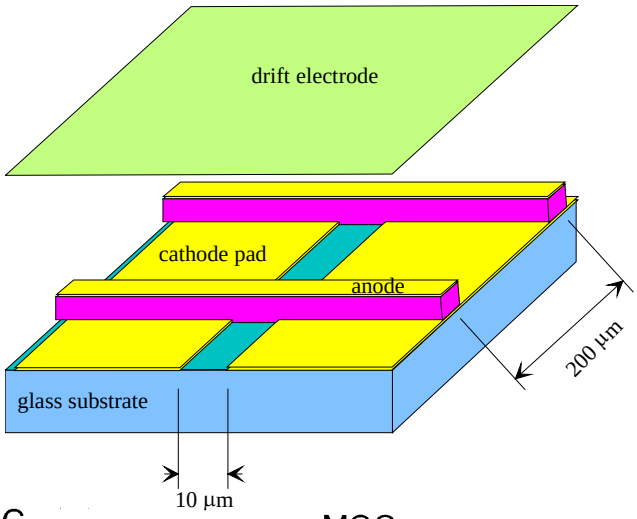

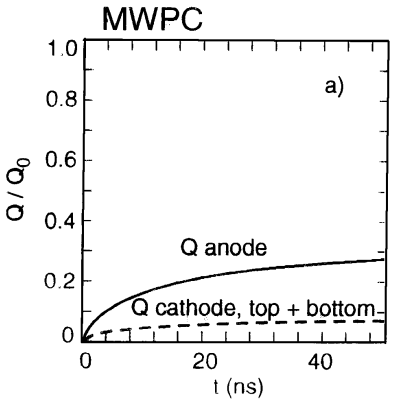

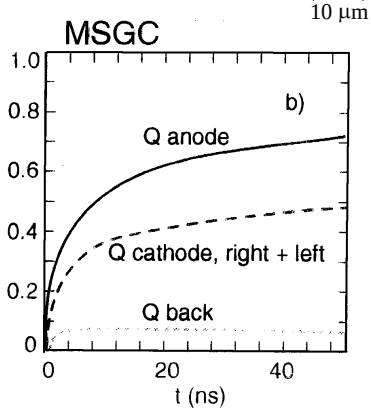

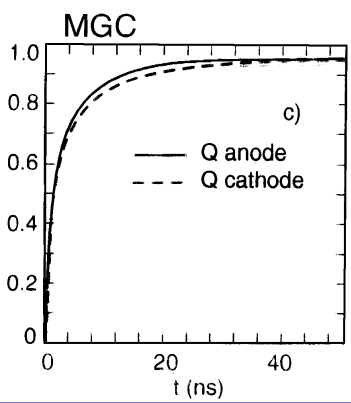

GEM: The Gas Electron Multiplier

(R. Bouclier et al., NIM A 396 (1997) 50)

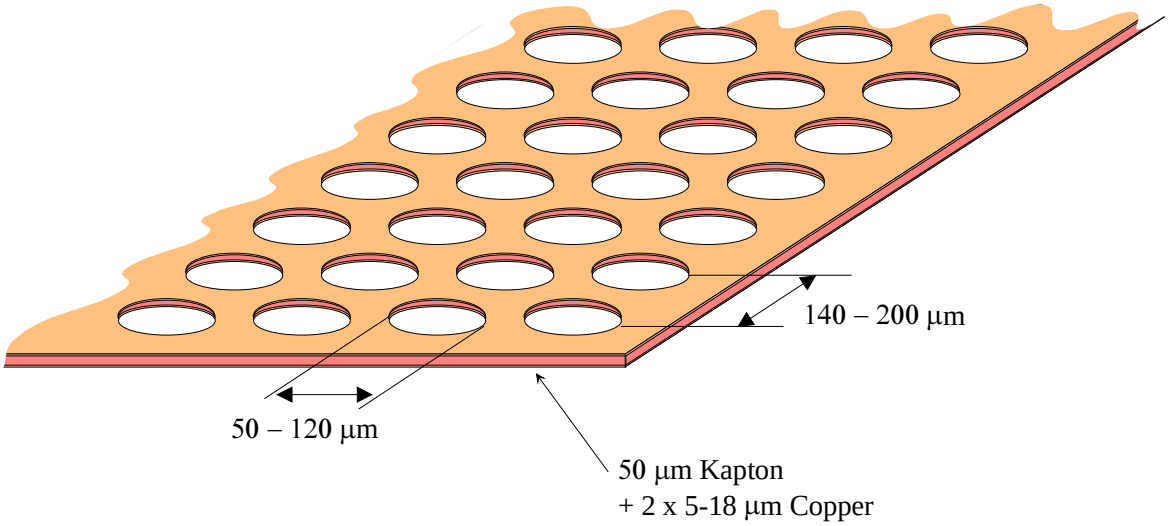

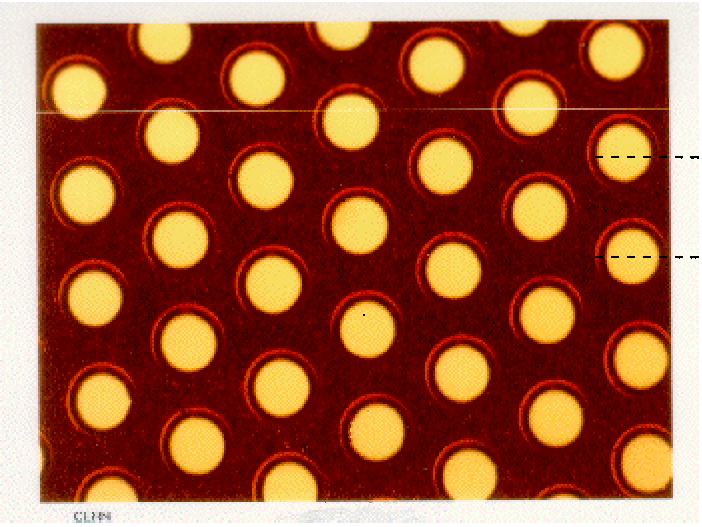

Micro photo of a GEM foil

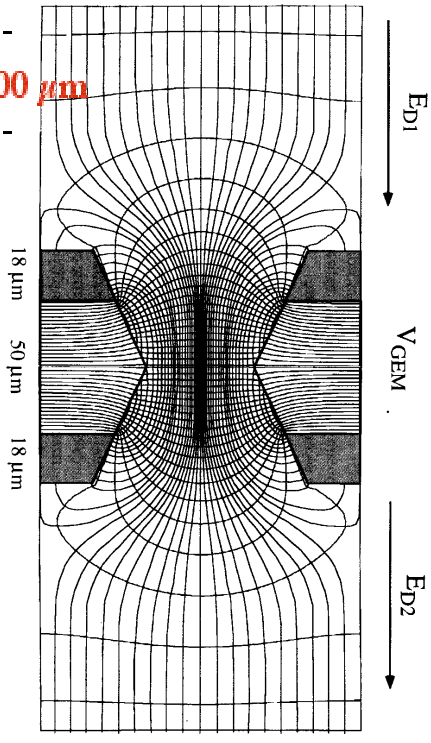

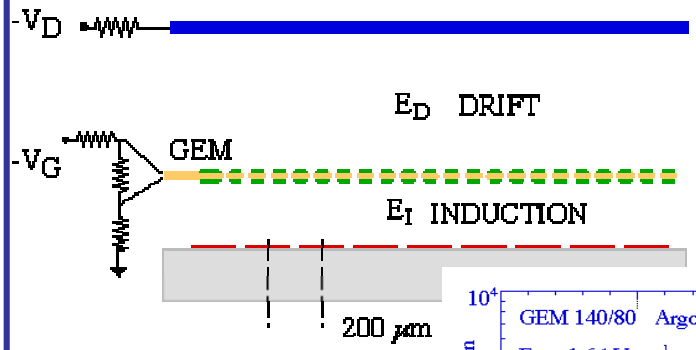

Single GEM
+ readout pads

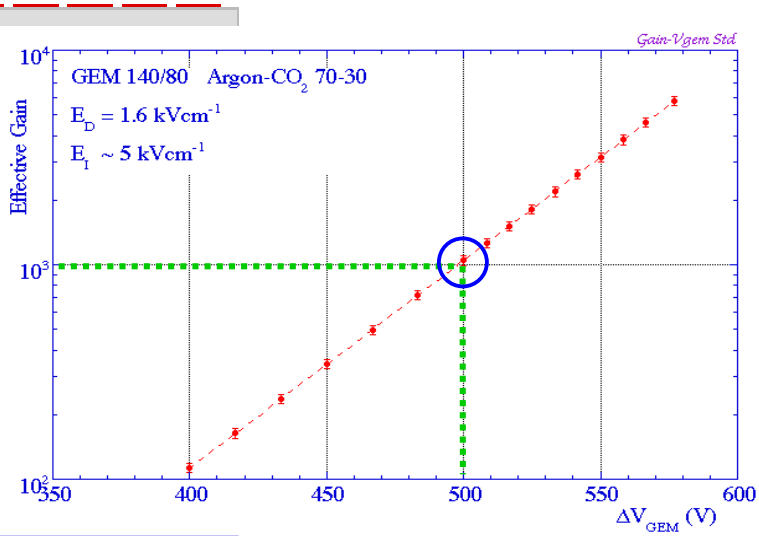

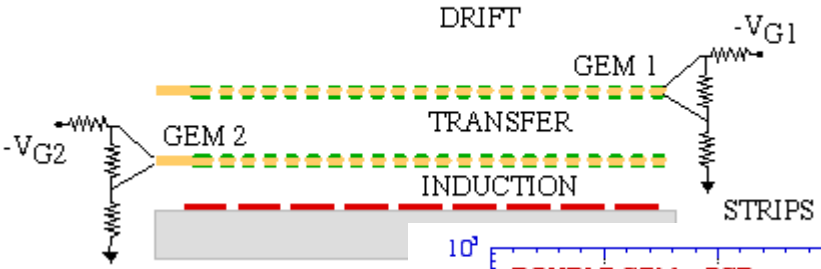

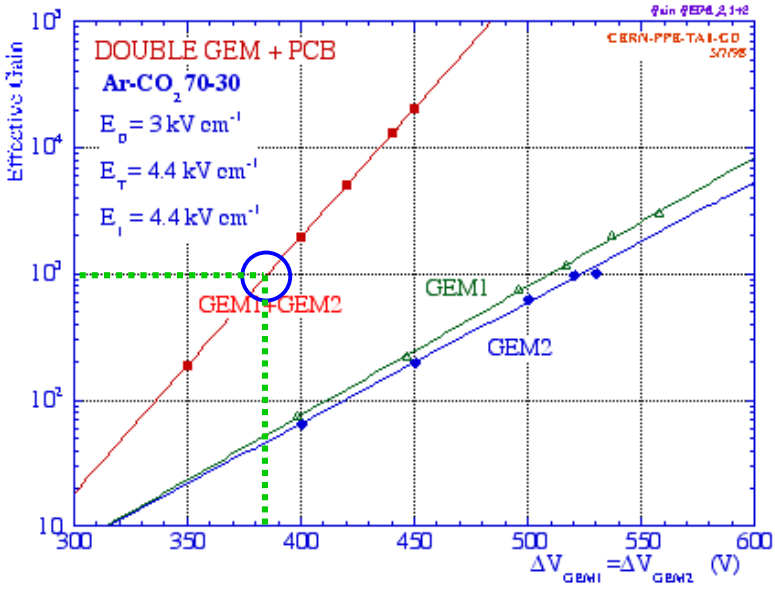

Double GEM
+ readout pads

- Same gain at lower voltage
- Less discharges

Micro Gap Wire Chamber

(E. Christophel et al., NIM A 398 (1997) 195)

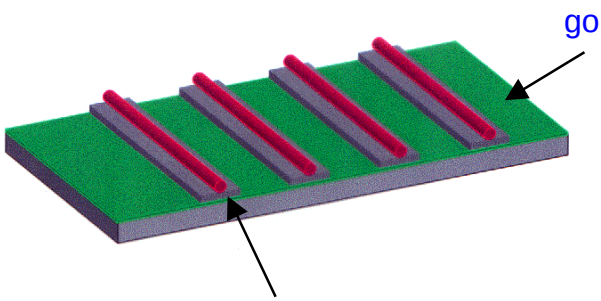

Gain > 10^5 (prototype 2.6 x 2.6 cm^2)

MICROMEGAS

(G. Charpak et al., CERN-LHC/97-08)

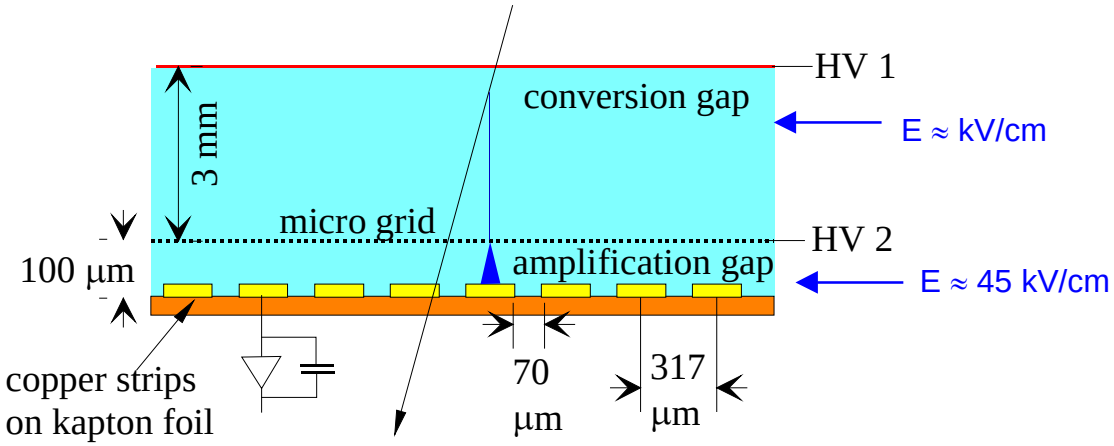

Gas: Ar-DME (≈80:20)

High rate capability (10^9 /(mm^2·s), prototype in test beam

Silicon detectors

Solid state detectors have a long tradition for energy measurements (Si, Ge, Ge(Li)).

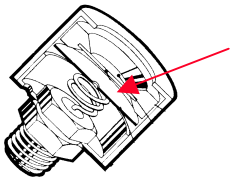

Si sensor

Here we are interested in their use as precision trackers !

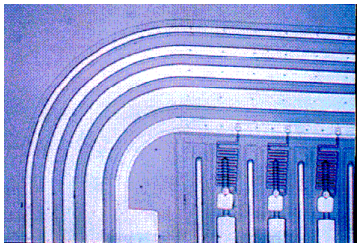

ATLAS SCT

Some characteristic numbers for silicon

- Band gap: E_g =1.12 V.
- E(e^--hole pair) = 3.6 eV, (≈ 30 eV for gas detectors).
- High specific density (2.33 g/cm^3) → ΔE/track length for M.I.P.'s.: 390 eV/μm ≈ 108 e-h/ μm (average)
- High mobility: μ_e =1450 cm^2/Vs, μ_h = 450 cm^2/Vs
- Detector production by microelectronic techniques → small dimensions → fast charge collection (<10 ns).
- Rigidity of silicon allows thin self supporting structures. Typical thickness 300 μm → ≈ 3.2 ·10^4 e-h (average)
- But: No charge multiplication mechanism!

How to obtain a signal ?

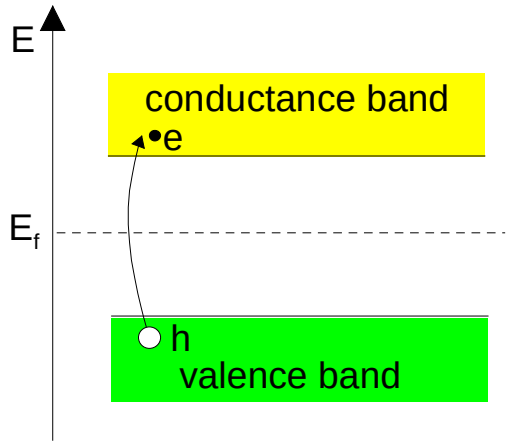

In a pure intrinsic (undoped) material the electron density n and hole density p are equal. $n = p = n_i$

For Silicon: $n_i \approx 1.45 \cdot 10^{10}$ cm^{-3}

In this volume we have $4.5 \cdot 10^8$ free charge carriers, but only $3.2 \cdot 10^4$ e-h pairs produced by a M.I.P.

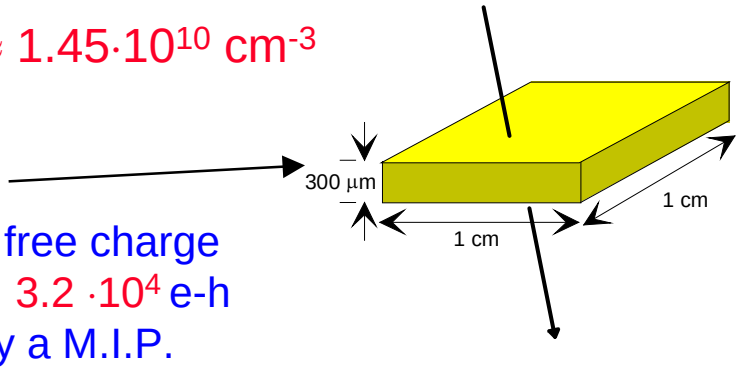

→ Reduce number of free charge carriers, i.e. deplete the detector

Most detectors make use of reverse biased p-n junctions

Doping

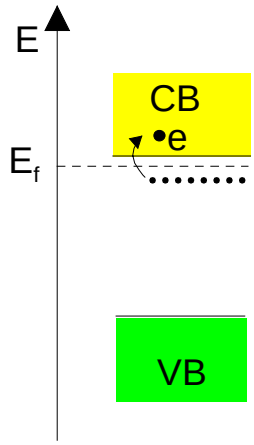

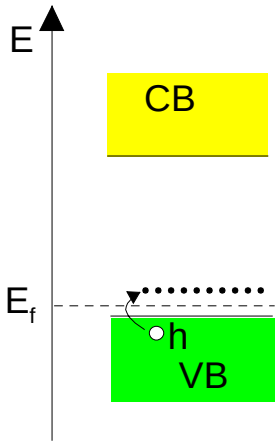

n-type: Add elements from Vth group, donors, e.g. As. Electrons are the majority carriers.

p-type: Add elements from IIIrd group, acceptors, e.g. B. Holes are the majority carriers.

	detector grade	electronics grade
doping concentration	10^{12} cm^{-3} (n) - 10^{15} cm^{-3} (p$^+$)	$10^{17(18)}$ cm^{-3}
resistivity	≈ 5 kΩ·cm	≈1 Ω·cm

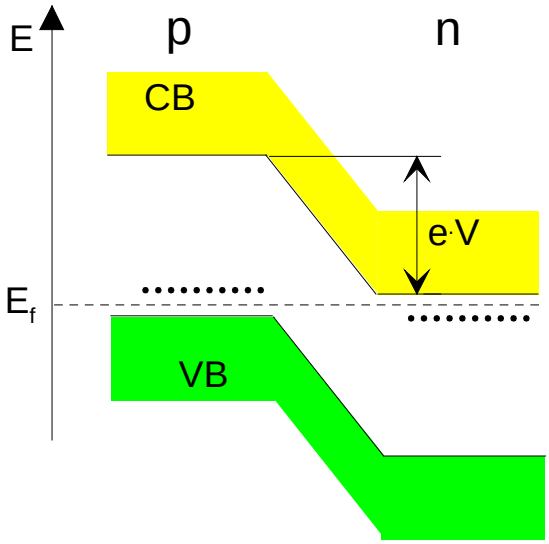

pn junction

There must be a single Fermi level !
Deformation of band structure → potential difference.

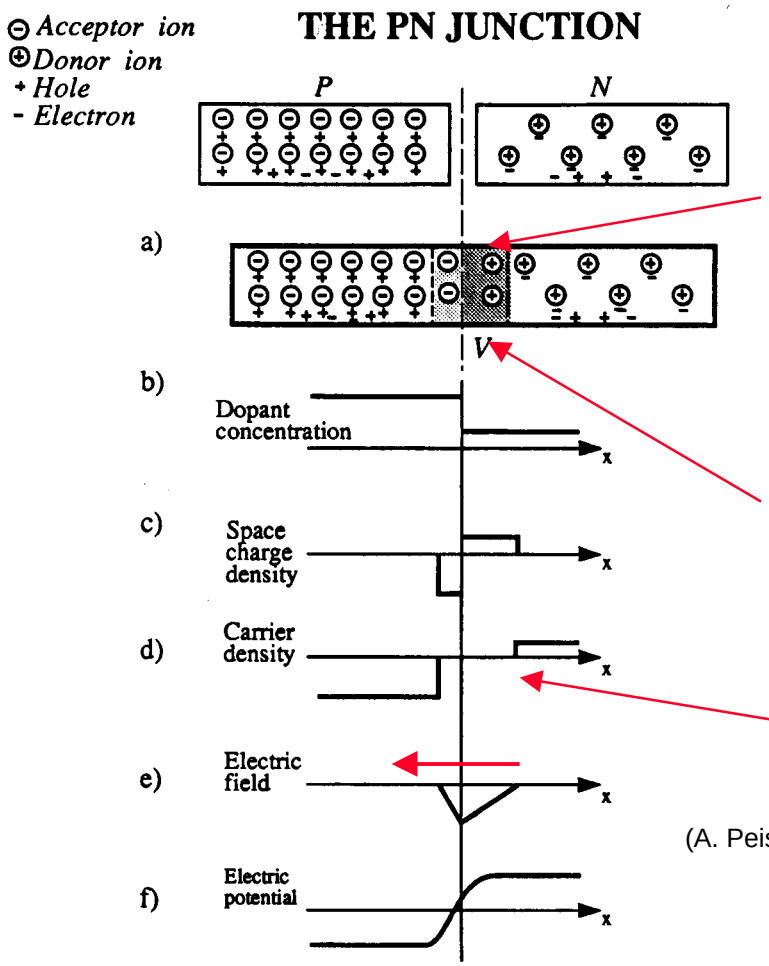

diffusion of e^- into p-zone, h^+ into n-zone → potential difference stopping diffusion

thin depletion zone

no free charge carriers in depletion zone

(A. Peisert, Instrumentation In High Energy Physics, World Scientific)

- Application of a reverse bias voltage (about 100V) → the thin depletion zone gets extended over the full junction → fully depleted detector.
- Energy deposition in the depleted zone, due to traversing charged particles or photons (X-rays), creates free e^--hole pairs.
- Under the influence of the E-field, the electrons drift towards the n-side, the holes towards the p-side → detectable current.

Spatial information by segmenting the p doped layer → single sided microstrip detector.

Schematically !

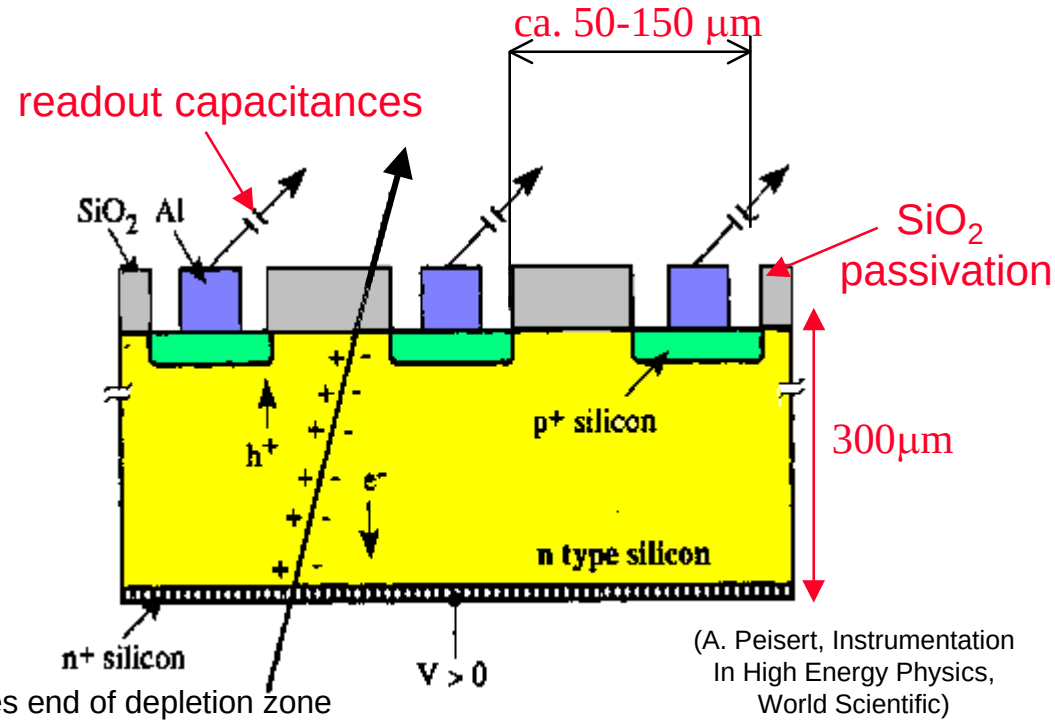

(A. Peisert, Instrumentation In High Energy Physics, World Scientific)

defines end of depletion zone
+ good ohmic contact

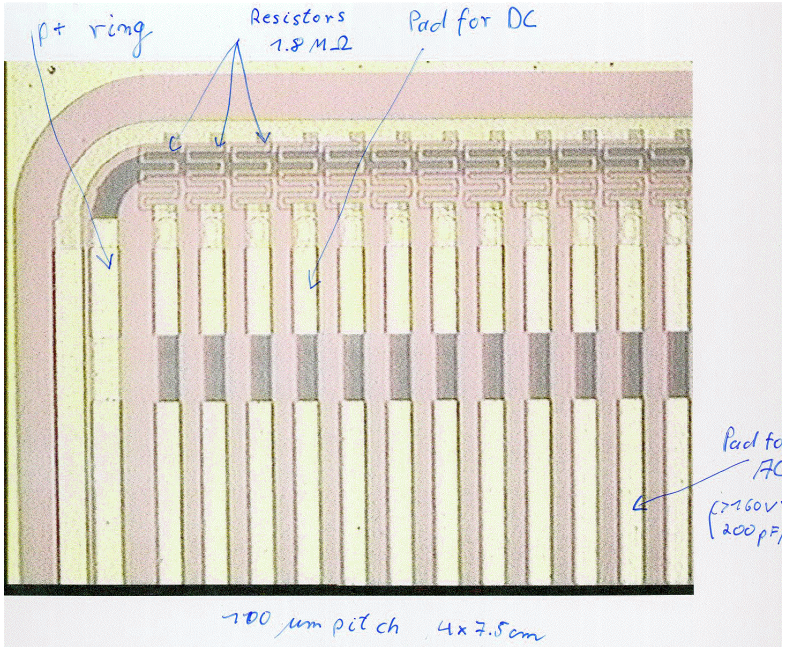

ALICE: Single sided micro strip prototype

Segmenting also the n doped layer → Double sided microstrip detector.

But:

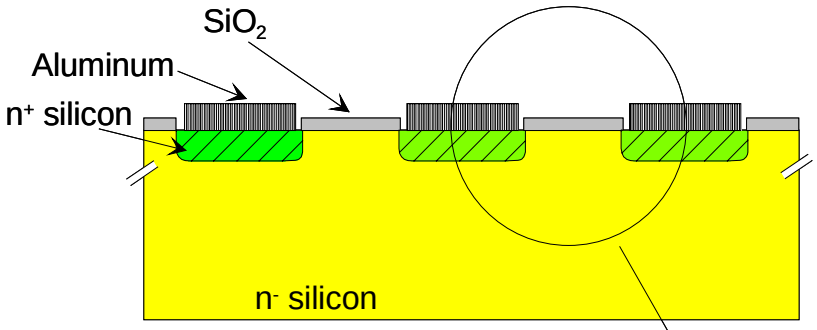

Positive charges in SiO_2 attract e^- in n^- layer. Short circuits between n^+ strips.

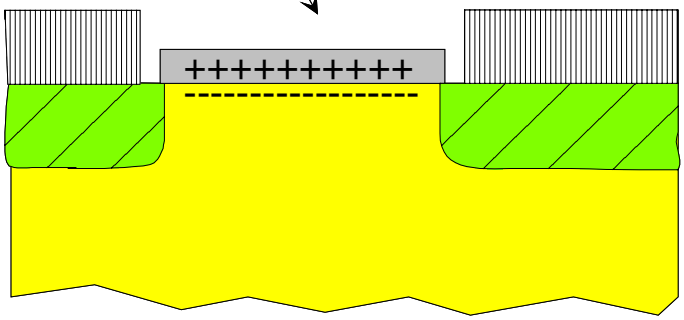

Two solutions:

Add p^+ doped blocking strips

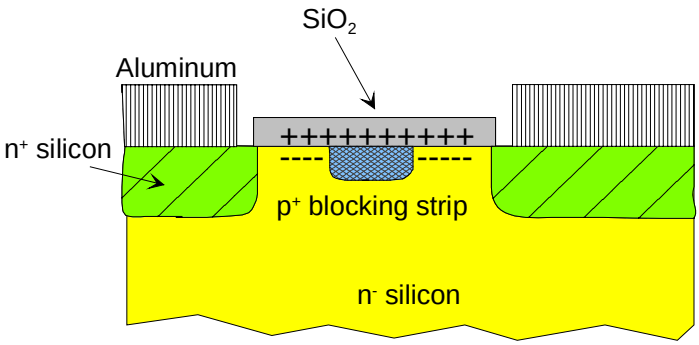

Add Aluminum layer on top of SiO_2
Negative biased MOS (metal oxide semiconductor) structure repelling e^-

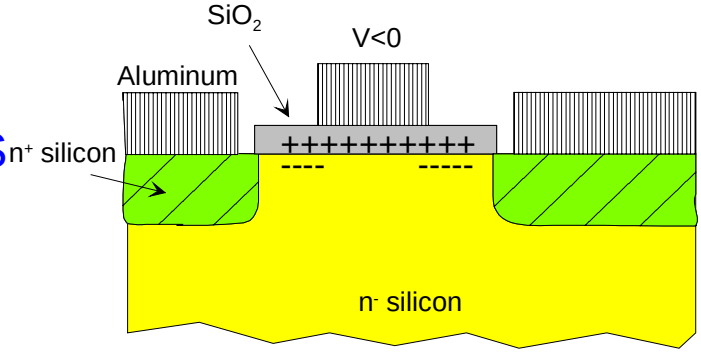

Silicon pixel detectors

- Segment silicon to diode matrix
- also readout electronic with same geometry
- connection by bump bonding techniques

Flip-chip technique

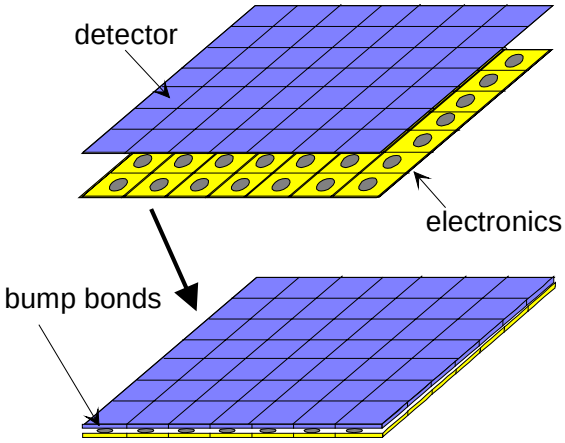

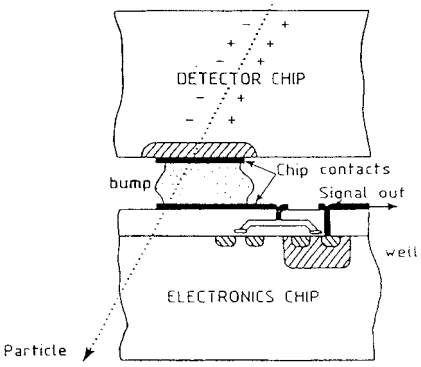

RD 19, E. Heijne et al., NIM A 384 (1994) 399

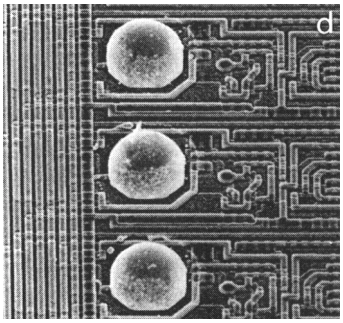

- Requires sophisticated readout architecture
- First experiment WA94 (1991), WA97
- OMEGA 3 / LHC1 chip (2048 pixels, 50x500 μm^2) (CERN ECP/96-03)
- Pixel detectors will be used also in LHC experiments (ATLAS, ALICE, CMS)

The DELPHI micro vertex detector (since 1996)

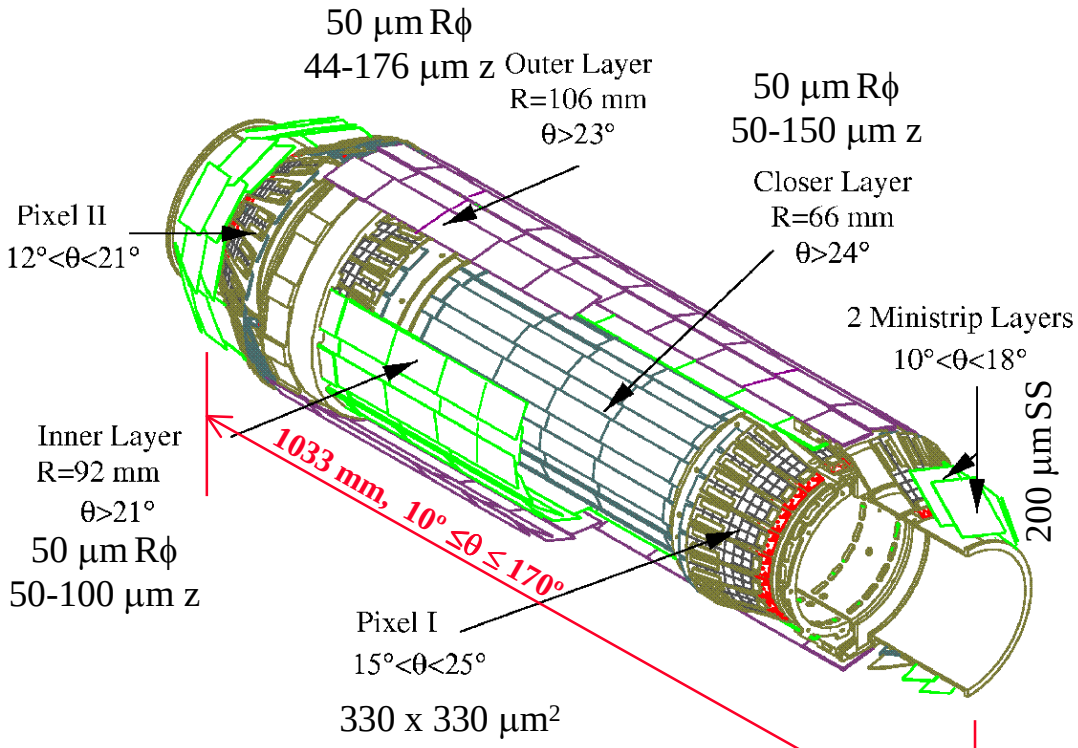

readout channels
ca. 174 k strips, 1.2 M pixels
total readout time: 1.6 ms

Total dissipated power 400 W
→ water cooling system

Hit resolution in barrel part ≈ 10 μm
Impact parameter resolution (rϕ)

$$28\mu m \oplus 71/\left(p\sin^{\frac{3}{2}}\theta \right)$$

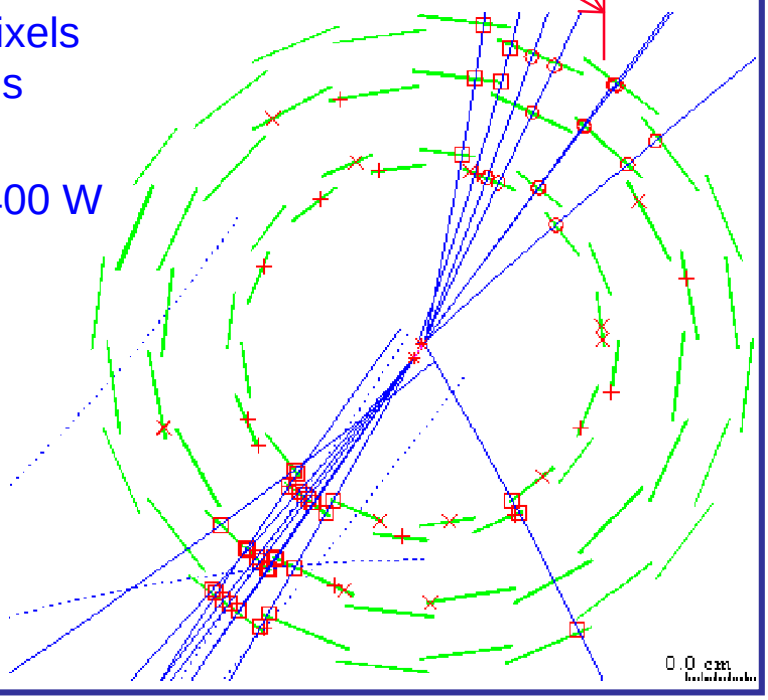

◆ Silicon drift chamber

(First proposed by E. Gatti and P. Rehak, NIM 255 (1984) 608)

principle:

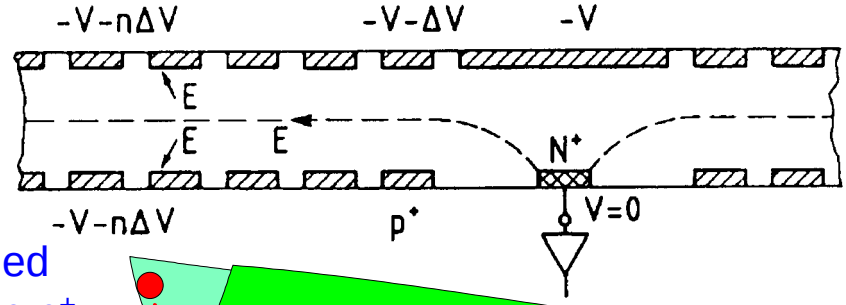

Define graded potentials on p^+ implants. Measure arrival time at n^+ strip

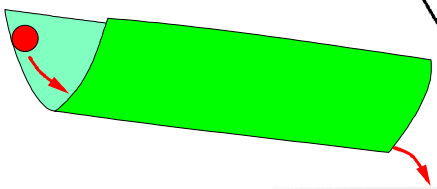

Segmentation of n^+ strip into pads → 2-D readout

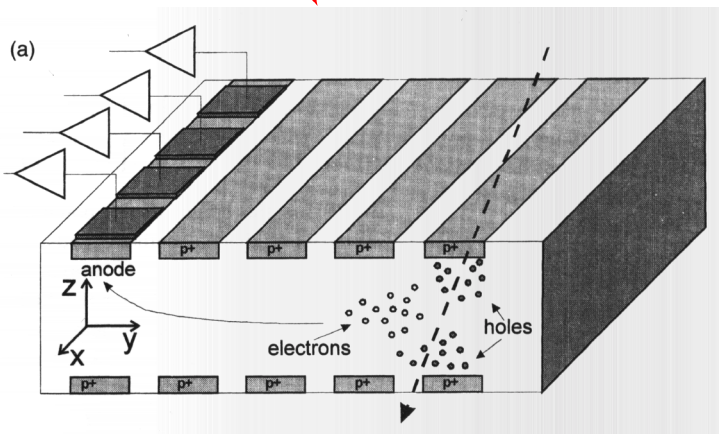

CERES (NA45): doublet of 3'' radial Si drift chambers

Intrinsic resolution:
$\sigma_R \approx 20\ \mu m$, $\sigma_\phi \approx 2$ mrad

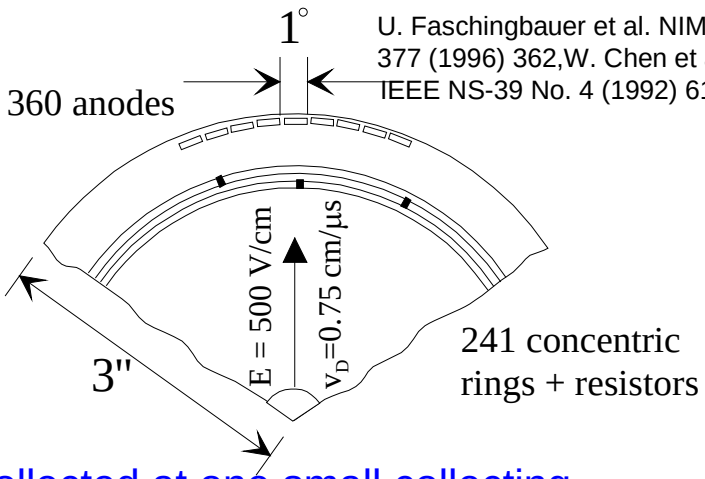

U. Faschingbauer et al. NIM A 377 (1996) 362,W. Chen et al, IEEE NS-39 No. 4 (1992) 619

The whole charge is collected at one small collecting electrode. Small capacity (100 fF) → low noise.

Monolithic integration of detector and electronics

Motivation:
- reduce strip or pixel dimensions
- avoid connection problems (bonding)
- improve performance (capacity, noise)
- reduce number of components

But silicon quality is very different for detectors and electronics !

2 possibilities:

1) build special electronics components on detector wafers

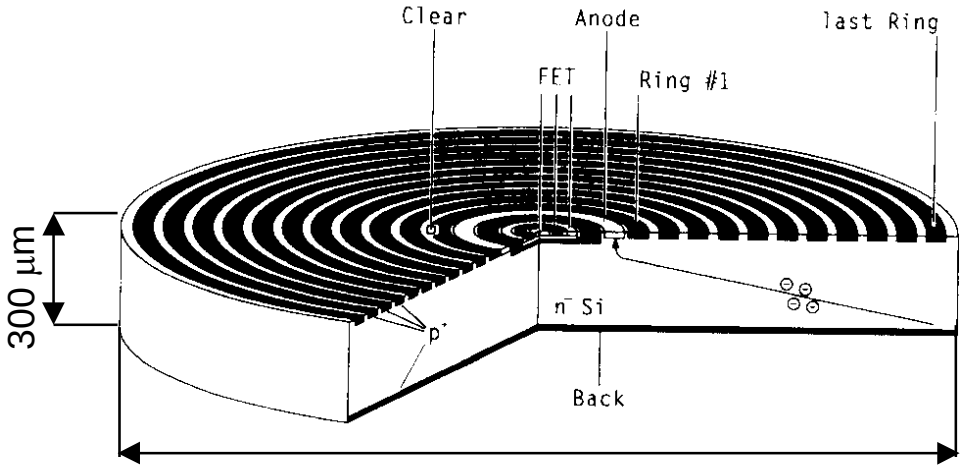

P. Lechner et al. NIM A 377 (1996) 346

2) grow detector grade silicon on electronics wafers

MIMOSA concept

J.D. Berst et al.
LEPSI -99-15

Y. Gormuskin et al.,
VCI 2001
submitted to NIM A

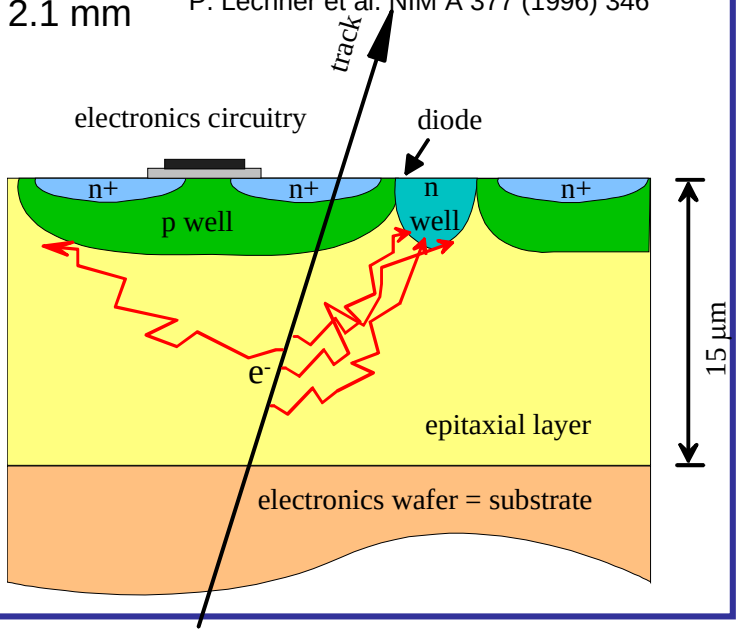

Radiation damage in silicon sensors

A major issue for LHC detectors !

Some definitions

- fluence: $\Phi = N/A$ [cm^{-2}]
- dose: D = E/m [Gy = J/kg]

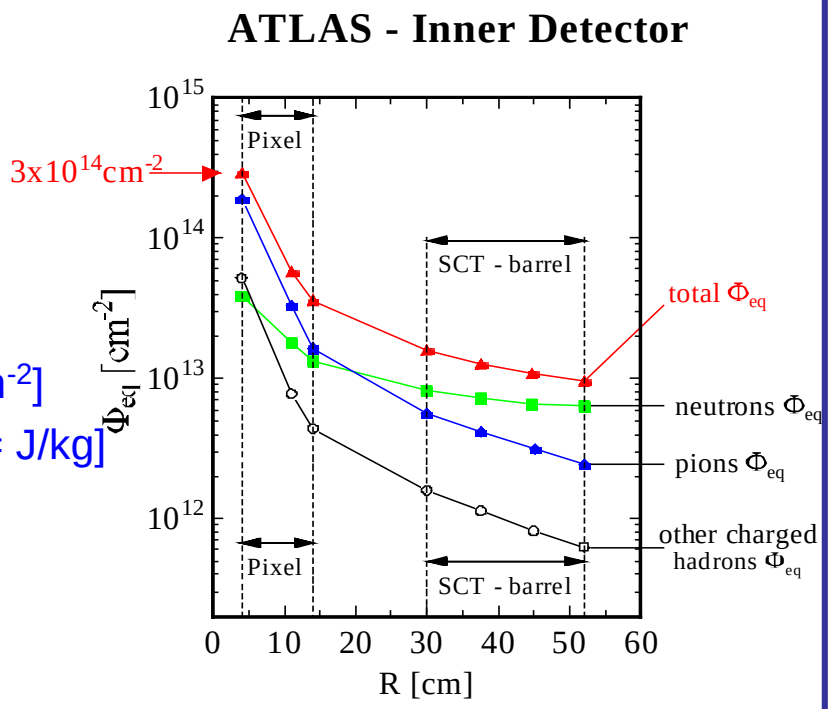

However: Specification of absorbed dose / fluence is not sufficient. Damage depends both on particle type (e,π,n, γ..) and energy !

Many effects and parameters involved (not all well understood)!

Damage caused by Non Ionising Energy Loss

Bulk effects: Lattice damage, vacancies and interstitials.

Surface effects: Oxide trap charges, interface traps.

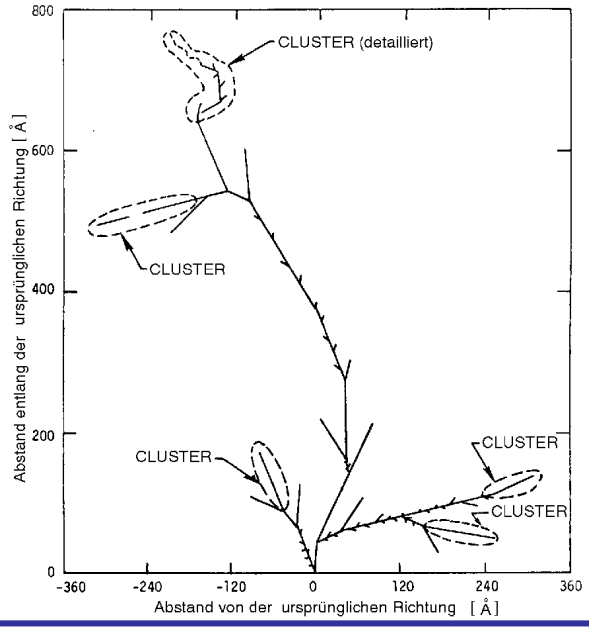

NIEL hypothesis (not fully valid !):

damage ∝ energy deposition in displacing collisions

Rel. damage function (normalized to neutrons of 1 MeV)

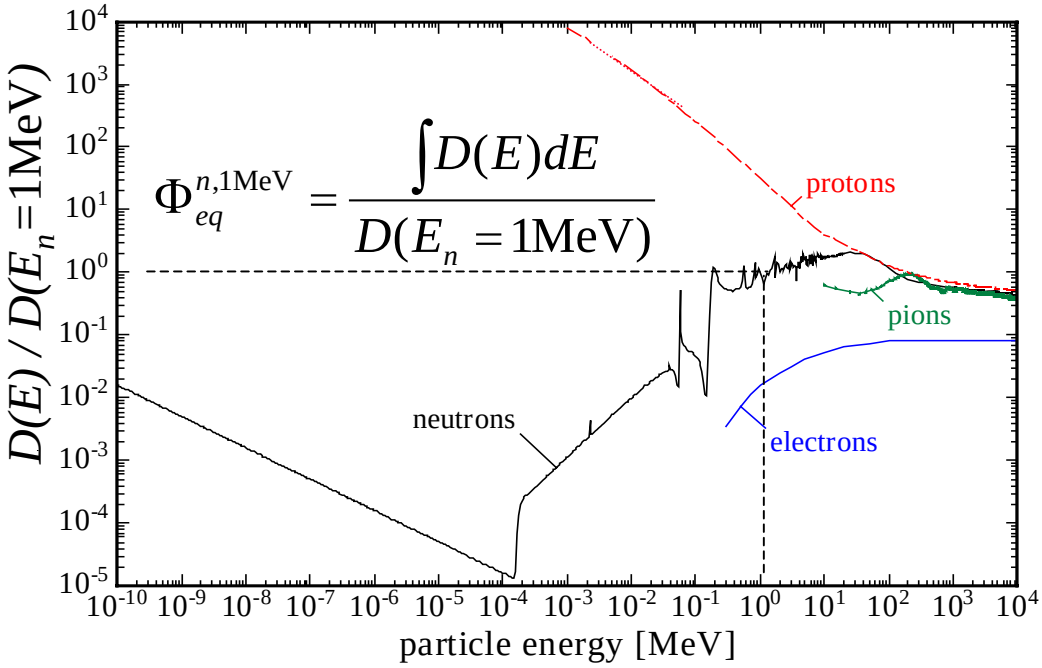

Main radiation induced macroscopic changes:

1. Increase of sensor leakage current

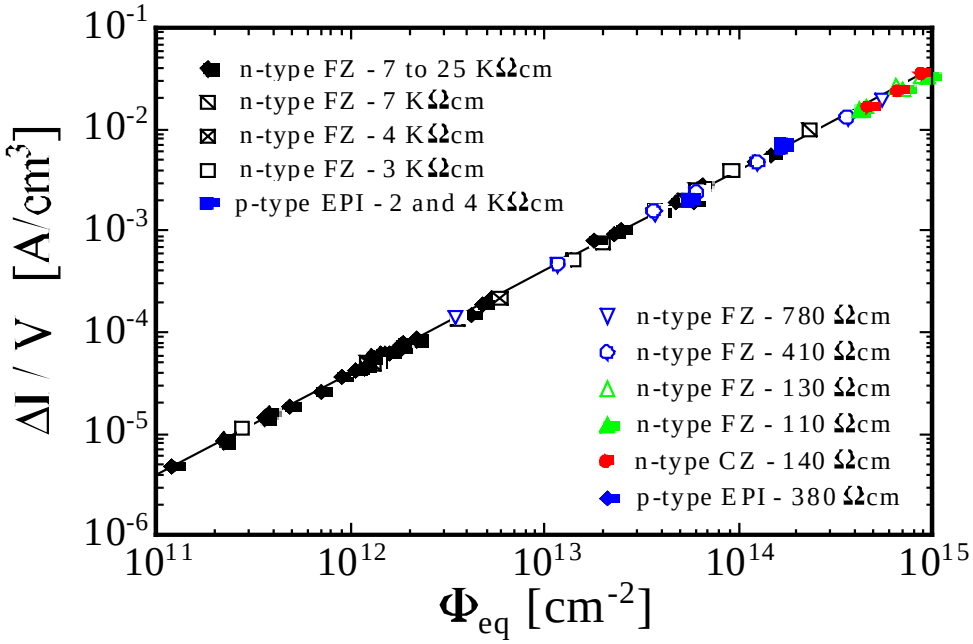

2. Change of depletion voltage. Very problematic.

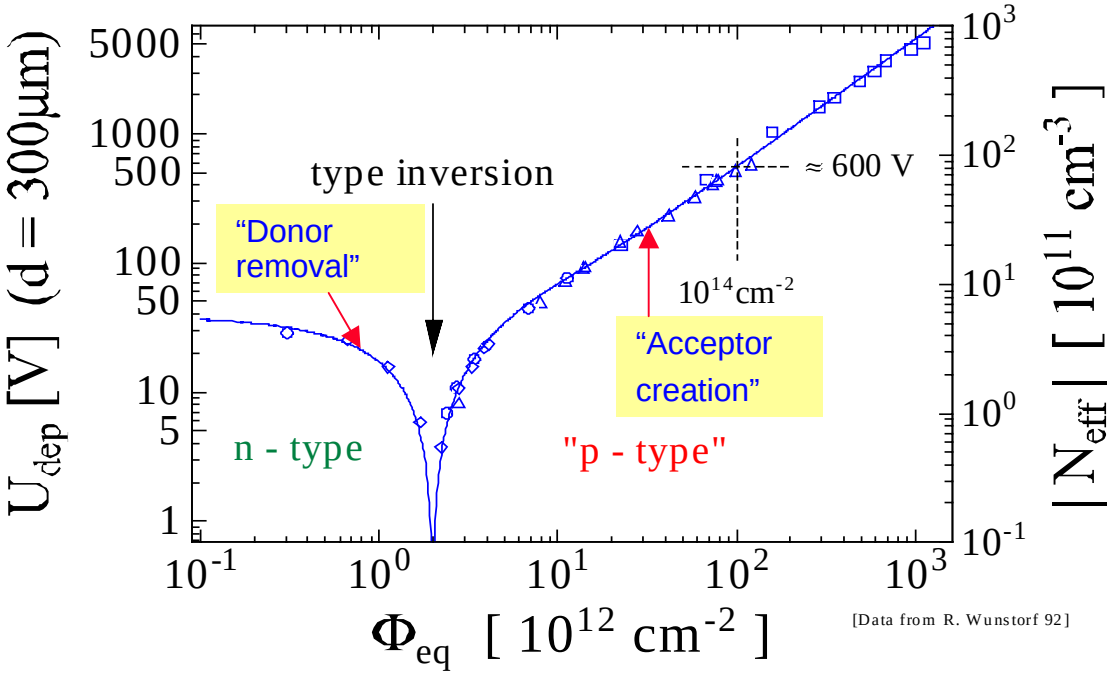

3. Decrease of the charge collection efficiency

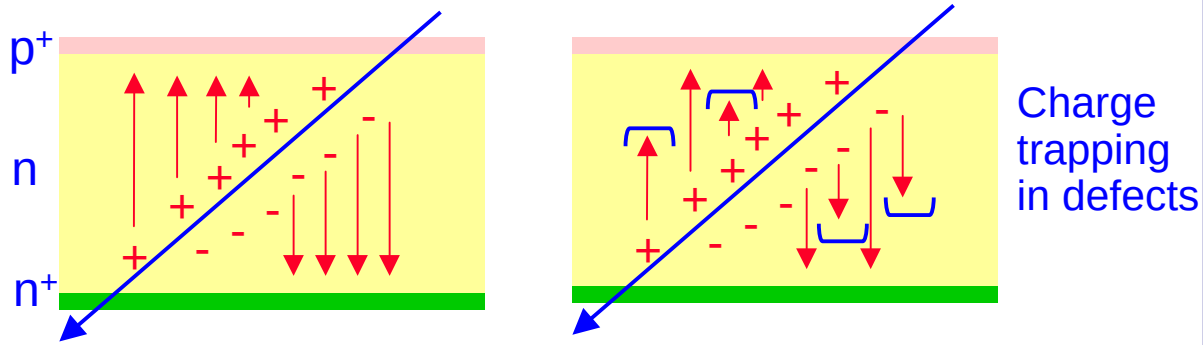

How to cope with the radiation damage ?

Possible strategies:

- Geometrical: build sensors such that they stand high depletion voltage (500V)
- Environmental: keep sensors at low temperature (≈ -10ºC).

→ Slower reverse annealing. Lower leakage current.

More advanced methods

ROSE / RD48
http://cern.ch/rd48

- **Defect engineering.**

  Introduce specific impurities in silicon, to influence defect formation. Example Oxygen.

  Diffusion Float Zone Oxyenated (DOFZ) silicon used in ATLAS pixel detector. Gain a factor 3.

RD39
http://cern.ch/rd39

- **Cool detectors to cryogenic temperatures** (optimum around 130 k)

  "zero" leakage current, good charge collection (70%) for heavily irradiated detectors ($1 \cdot 10^{15}$ n/cm^2). "Lazarus effect"

RD42
http://cern.ch/rd42

- **New materials**

  Diamond. Grown by Chemical Vapor Deposition. Very large bandgap (≈ 6 eV). No doping required and depletion required! Material is still rather expensive. Still more R&D required.

- **New detector concepts**

  "3D detectors" → "horizontal" biasing

  faster charge collection

  but difficult fabrication process